



OPEN

## Synthesis of coumarin derivatives and investigation of their inhibitory effects on lung cancer cell motility

Rui Zhou, Young Hyun Yu, Hangun Kim & Hyung-Ho Ha

Based on the pharmaceutical potentials of coumarins, which have antitumor activity, we synthesized new coumarin derivatives and evaluated their biological activities. The new coumarin derivatives were chemically synthesized from 4-hydroxycoumarin, and their structures were confirmed by nuclear magnetic resonance data. Ten of the synthesized compounds were investigated for antimetastatic activity against lung carcinoma cells. Several of the tested compounds showed good to mild inhibitory effects on lung cancer cell motility. There were no cytotoxic effects related to the use of these compounds. 4-Hydroxycoumarin derivatives, 4h and 4i, elicited the significant inhibitory effect on lung cancer cell motility by suppressing expression of the epithelial–mesenchymal transition markers N-cadherin, Snail, and Twist.

Lung adenocarcinoma is the most malignant diagnosed cancer and is the leading cause of cancer death in men worldwide, followed by colorectal and liver cancer<sup>1,2</sup>. Lung cancer has various preferential sites for metastasis, such as the liver, brain, and bones<sup>3</sup>. Patients with metastatic lung adenocarcinoma have a poor prognosis and usually survive for fewer than 5 years<sup>4</sup>. The epithelial–mesenchymal transition (EMT) is a common mechanism underlying lung cancer cell motility and progression<sup>5</sup>. It facilitates metastasis by promoting lung cancer cell invasion, migration, and resistance to apoptotic stimuli. Therefore, inhibition of the EMT suppresses metastasis and progression of lung cancer<sup>6</sup>.

Coumarins, which are well-known condensed benzoheterocycles, are used as medicinal chemicals because they are easily synthetically transformed into a large variety of functionalized structures<sup>7</sup>. They have various purposes, such as synthesis of medicines<sup>8</sup>; laser dyes; and compounds with antifungal<sup>9</sup>, antibacterial<sup>10</sup>, anti-inflammatory<sup>11</sup>, and anticancer activities<sup>11,12</sup>. Recently, coumarin derivatives were reported to have inhibitory effects on prostate cancer, colon cancer, gastric cancer, and pancreatic cancer, mainly by regulating cell proliferation and apoptosis. Coumarin derivative esculetin inhibits the proliferation of human prostate cancer cells by inducing apoptosis and arresting the cell cycle<sup>13</sup>. 5-Geranyloxy-7-methoxycoumarin inhibits colon cancer cell growth via induction of apoptosis<sup>14</sup>. Coumarin-indole derivative MY-413 induces gastric cancer cell apoptosis and inhibits proliferation through MAPK signaling pathway<sup>15</sup>. Coumarin derivatives (12a–x) functions as NEDD8 activating enzyme inhibitors and induces apoptosis in pancreatic cancer cells<sup>16</sup>. Due to their many uses, it has become important to synthesize coumarins or their derivatives with conventional drugs by various reactions<sup>17,18</sup>. Various synthetic methods for coumarins and their derivatives have been used to insert various substituents into specific areas of the coumarin structure, thereby allowing mechanistic exploration of their anticancer activities. Herein, we summarize the inhibitory effects of coumarin derivatives on lung cancer cell motility.

### Results and discussion

**Chemistry.** 4-Hydroxycoumarin is an effective drug for small cell lung cancer<sup>15</sup>. Therefore, we used 4-hydroxycoumarin as a material to chemically synthesize 3-nitro-4-hydroxycoumarin (**2**) in the presence of HNO<sub>3</sub> at 60 °C in an oil bath and then 3-amino-4-hydroxycoumarin (**3**) in the presence of Pd/C, and in a H<sub>2</sub> atmosphere for 8 h (Fig. 1).

3-Amino-4-hydroxycoumarin (**3**) has an amino group (NH<sub>2</sub>), which is a stable functional site. Various substituted acid chlorides (**4a–4j**) were selected as the linker via a carboxyl group (–COOH). Ten 3-amidocoumarins (**4a–4j**) were synthesized by a reaction involving formation of a peptide bond (–CO–NH–). A peptide bond was used due to its resonance stabilization and readiness to undergo chemical reactions. The structures of different aminocoumarin derivatives are presented in Fig. 2.

College of Pharmacy, Suncheon National University, 255 Jungang-Ro, Suncheon, Jeonnam 57922, Republic of Korea.  
✉ email: hangunkim@sunchon.ac.kr; hhha@sunchon.ac.kr

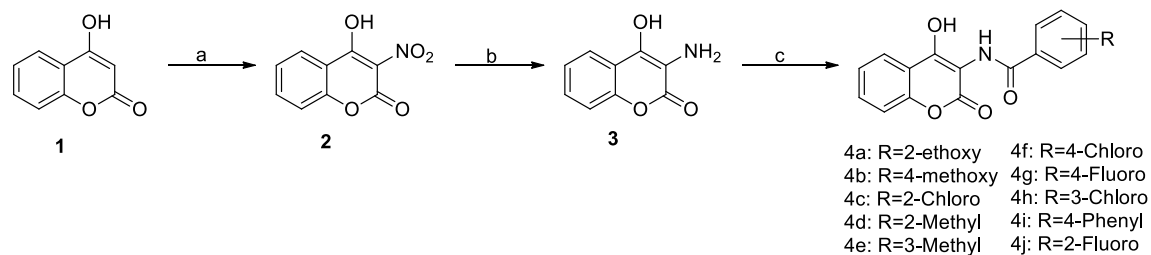


**Figure 1.** Synthesis pathway of coumarin analogues. Reagents and conditions: (a)  $\text{HNO}_3$ ,  $\text{NaNO}_2$ ,  $\text{AcOH}$ , 1 h,  $60^\circ\text{C}$ ; (b)  $\text{H}_2$ ,  $\text{Pd/C}$ ,  $\text{EtOH}$ , 8 h, rt; (c) Benzoyl chloride, Pyridine,  $\text{CH}_2\text{Cl}_2$ , 8 h, rt.

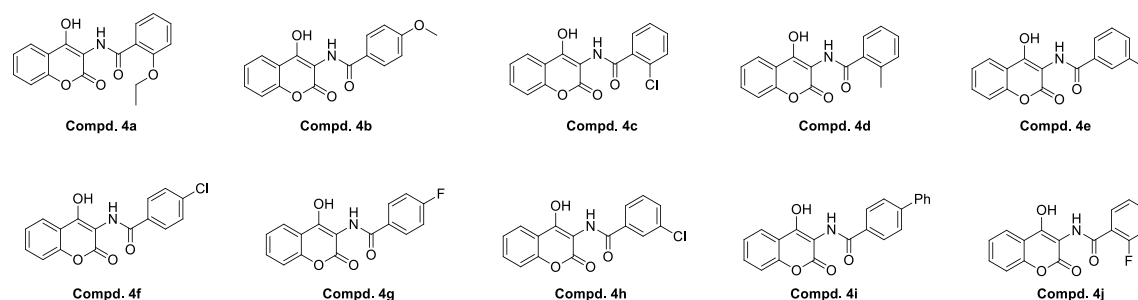


**Figure 2.** Structure of Aminocoumarin derivatives (4a–4j).

**Biological evaluation.** Cancer metastasis accounts for much of the morbidity and is associated with ~90% of the cancer-associated deaths<sup>19</sup>. According to the GLOBOCAN analysis, lung cancer is one of the most malignant types with metastasis, with a higher mortality rate of around 18.4%<sup>20</sup>. The motility of cancer cells contributes to tumor metastasis with several stages, including invading across the basement membranes, migration to blood, intravasation and movement into distant organs<sup>21</sup>. Cell migration and invasion are relevant phenotypes when studying the effect of novel therapeutic drugs against metastasis in cancer development and progression<sup>22</sup>. This study aimed to elucidate whether chemically synthesized coumarin derivatives affect lung cancer cell motility. To determine the cytotoxic effects of all the compounds on lung cancer cells, viability of A549, H460, and H1975 cells were evaluated via the MTT assays. Treatment with 3.125–20  $\mu\text{M}$  of 4-hydroxycoumarin and its derivatives 4a–4j did not affect the viabilities of A549, H460, and H1975 cells. Treatment with 50–100  $\mu\text{M}$  of 4-hydroxycoumarin and its derivatives 4a–4j inhibited the cell viabilities by ~25% in A549, H460, and H1975 cells (Fig. 3a and Supplementary Fig. S1). An invasion assay was performed to examine their effects on A549 cell motility. Cells were treated with 4-hydroxycoumarin and its derivatives 4a–4j at nontoxic concentration of 5  $\mu\text{M}$  for 24 h. Treatment with compounds 4d, 4h, and 4i significantly inhibited A549 cell invasion by ~40%, ~50%, and ~40% ( $p < 0.0001$ ), respectively (Fig. 3b,c).

To elucidate how these three compounds inhibit cancer cell motility at noncytotoxic concentrations, cells were mainly treated with nontoxic concentrations at 5, 10, or 15  $\mu\text{M}$  of compounds 4d, 4h, and 4i in subsequent experiments. Treatment with compounds 4d, 4h, and 4i dose-dependently decreased the number of invaded A549 cells (Fig. 4).

Wound healing assays are a commonly used method to evaluate cell migration ability<sup>23</sup>. The wound healing assay was performed by treating A549 cells with 15  $\mu\text{M}$  compounds 4d, 4h, and 4i (Fig. 5). Cell migration was inhibited by treatment with compounds 4h and 4i in a time-dependent manner but was unaffected by compounds 4d treatment.

Moreover, the migration assay was performed using the other lung cancer cell lines H460, and H1650. Treatment with compounds 4h and 4i significantly decreased abilities of migrated cells in both cell lines (Fig. 6a,b). However, cell migration abilities of H460 and H1650 were also unaffected by treatment with compound 4d (Supplementary Fig. S2), indicating that it might not be a selection against lung cancer motility. The invasion assays were performed using H460, H1650, and H1975 cells. Treatment with compounds 4h and 4i significantly decreased numbers of invaded cells of all three cell lines by more than 25% ( $p < 0.005$ ) (Fig. 6c). Taken together, these results indicate that compounds 4h and 4i significantly suppress lung cancer cell motility.

The EMT plays a role in lung cancer cell motility and metastasis<sup>24</sup>. In the EMT process, epithelial cells lose cell–cell adhesion and decrease the expression of epithelial cells marker such as E-cadherin, inversely, the expression of mesenchymal cell markers such as N-cadherin is increased, associated with invasive phenotype<sup>25</sup>. Several reports have proved that loss of E-cadherin expression or induction of N-cadherin led to poor prognosis in lung cancer<sup>26–28</sup>. E-cadherin and N-cadherin, as well as their regulators Snail and Twist, are indicators of the EMT<sup>24</sup>. The protein and mRNA expression levels of these EMT markers and their regulators were examined to determine how compounds 4h and 4i suppress lung cancer cell motility. Treatment with 15  $\mu\text{M}$  compounds 4h decreased expression of not only N-cadherin but also E-cadherin and suppressed mRNA expression of Snail and Twist (Fig. 7a,c). Treatment with compound 4i significantly increased the expression of E-cadherin and downregulated the expression of N-cadherin, Snail, and Twist at a dose-dependent manner (Fig. 7b,d). These results indicate

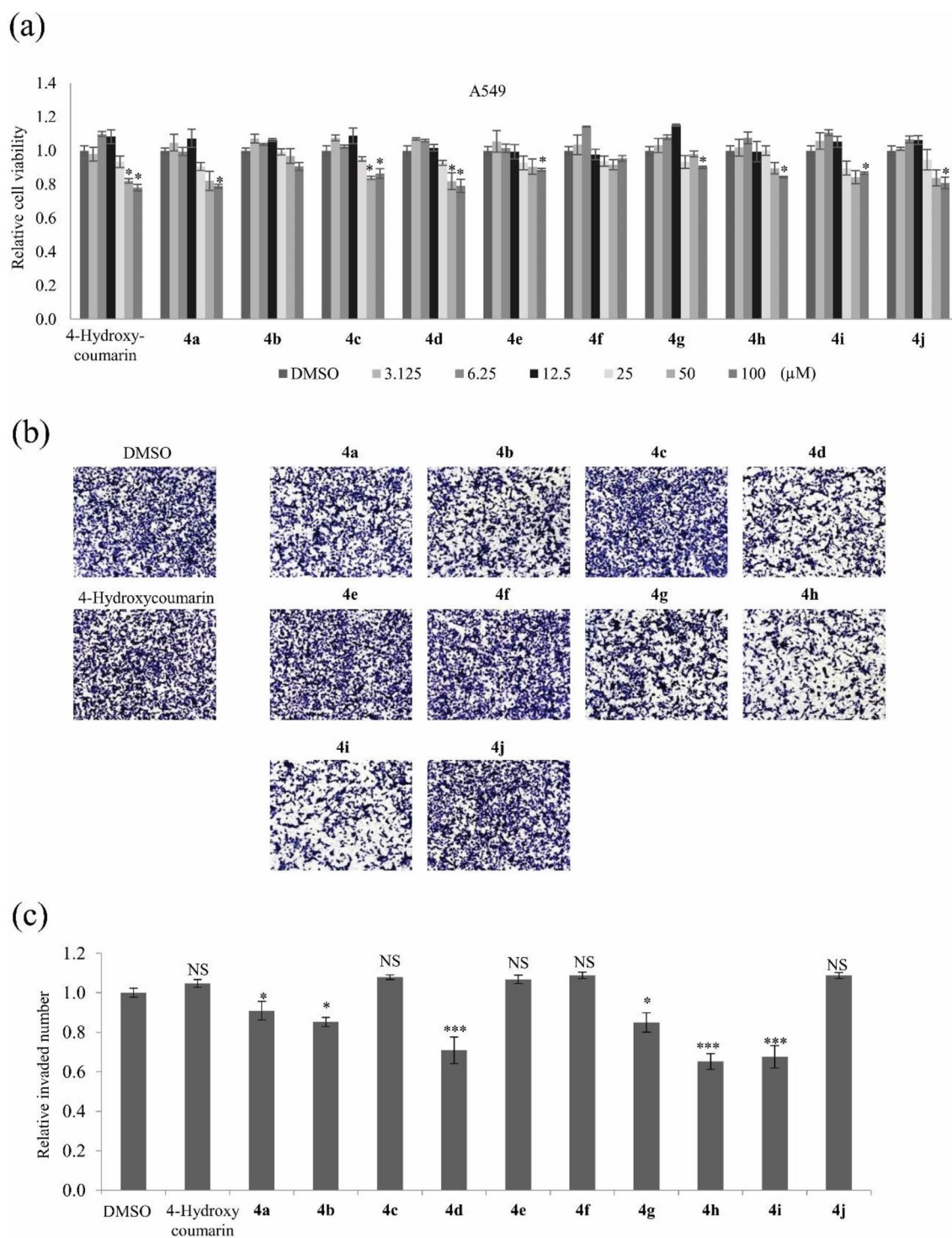


**Figure 3.** The effects of 4-hydroxycoumarin and its derivatives **4a–4j** on invasion of A549 cells. (a) Relative viabilities of A549 cells after treatment with 4-hydroxycoumarin and its derivatives **4a–4j** for 48 h at concentrations ranging from 3.125 to 100  $\mu\text{M}$  measured by the MTT assay. (b) Representative images of invasion assays of A549 cells treated with 4-hydroxycoumarin and its derivatives **4a–4j** at a concentration of 5  $\mu\text{M}$ . (c) Quantitative analysis of invaded cell numbers after each treatment. Representative images from three independent experiments are shown ( $n=3$ ). Data represent the mean  $\pm$  SD. \* $p < 0.05$ ; \*\*\* $p < 0.001$ ; NS, no significant difference compared with dimethyl sulfoxide (DMSO)-treated A549 cells.

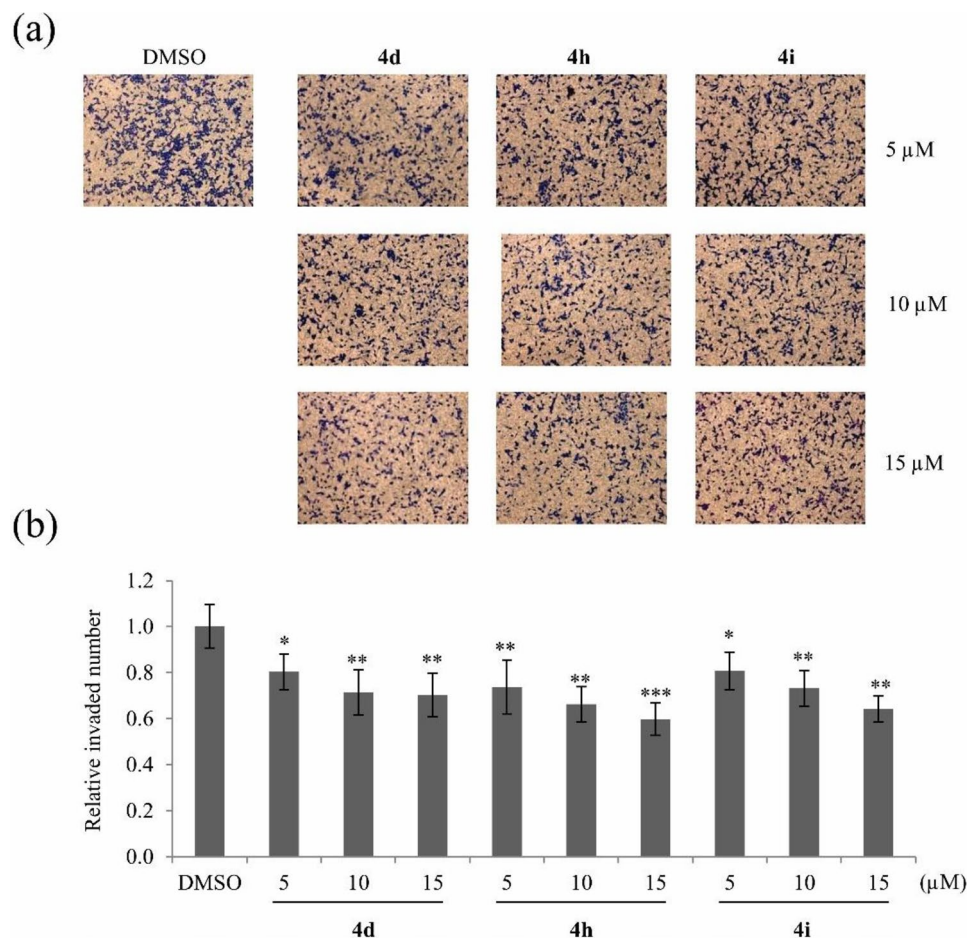


**Figure 4.** Suppression of A549 cell invasion by compounds **4d**, **4h**, and **4i**. (a) Representative images of invaded A549 cells after treatment with various nontoxic concentrations (5, 10, and 15  $\mu\text{M}$ ) of compounds **4d**, **4h**, and **4i** for 24 h. (b) Quantitative analysis of invaded cell numbers in each group. Representative images from three independent experiments are shown ( $n = 3$ ). Data represent the mean  $\pm$  SD. \* $p < 0.05$ ; \*\* $p < 0.01$ ; \*\*\* $p < 0.001$  compared with DMSO-treated A549 cells.

that compound **4i** inhibits expression of EMT markers more than compound **4h**. However, compound **4d** did not affect E/N-cadherin expression as shown in Supplementary Fig. S2c. Taken together, our data demonstrate that compounds **4h** and **4i** inhibit lung cancer cell motility by downregulating EMT markers.

## Conclusion

Ten amidocoumarin derivatives (**4a–4j**) were newly synthesized by a chemical reaction, and their inhibitory effects on lung carcinoma were evaluated. Compounds **4h** and **4i** inhibited invasion and migration of lung cancer cells by modulating expression of EMT effectors. Moreover, the inhibition of EMT markers by compound **4i** was highest, suggesting that it is a potential inhibitor of lung cancer motility. A further biological study is required to elucidate the detailed underlying molecular mechanism.

## Methodology

**Chemistry.** *Synthesis of 4-hydroxy-3-nitrocoumarin (2).* Commercially available 4-hydroxycoumarin (**1**, 3.24 g, 20 mmol, Aldrich) was dissolved in AcOH (60 mL). One portion of sodium nitrite (14 mg, 0.2 mmol) was added to this solution before  $\text{HNO}_3$  (3 mL) dropwise. The reaction was allowed to stir 10 min at room temperature, followed by heating at 60  $^\circ\text{C}$  for 1 h in an oil bath. The brown solution was allowed to attain to the room temperature and the pure compound crystallized out from the solution. The suspension was filtered and washed with hexane, and then dried to afford 3-nitro-4-hydroxycoumarin (**2**) as off-yellow crystals. 3.5 g; yield 85%.

*Synthesis of 3-amino-4-hydroxycoumarin (3).* 4-Hydroxy-3-nitrocoumarin (**2**, 3.1 g, 15 mmol) was dissolved in EtOH, and a catalytic amount of Pd/C (30 mg) was added to the mixture at room temperature. The resulting solution was stirred at room temperature under  $\text{H}_2$  atmosphere for 5 h. After completion of the reaction, the mixture was filtered to remove the catalyst with celite pad, washed with MeOH and ethyl acetate, and concentrated to afford an off-white solid. 2.3 g; yield 87%.



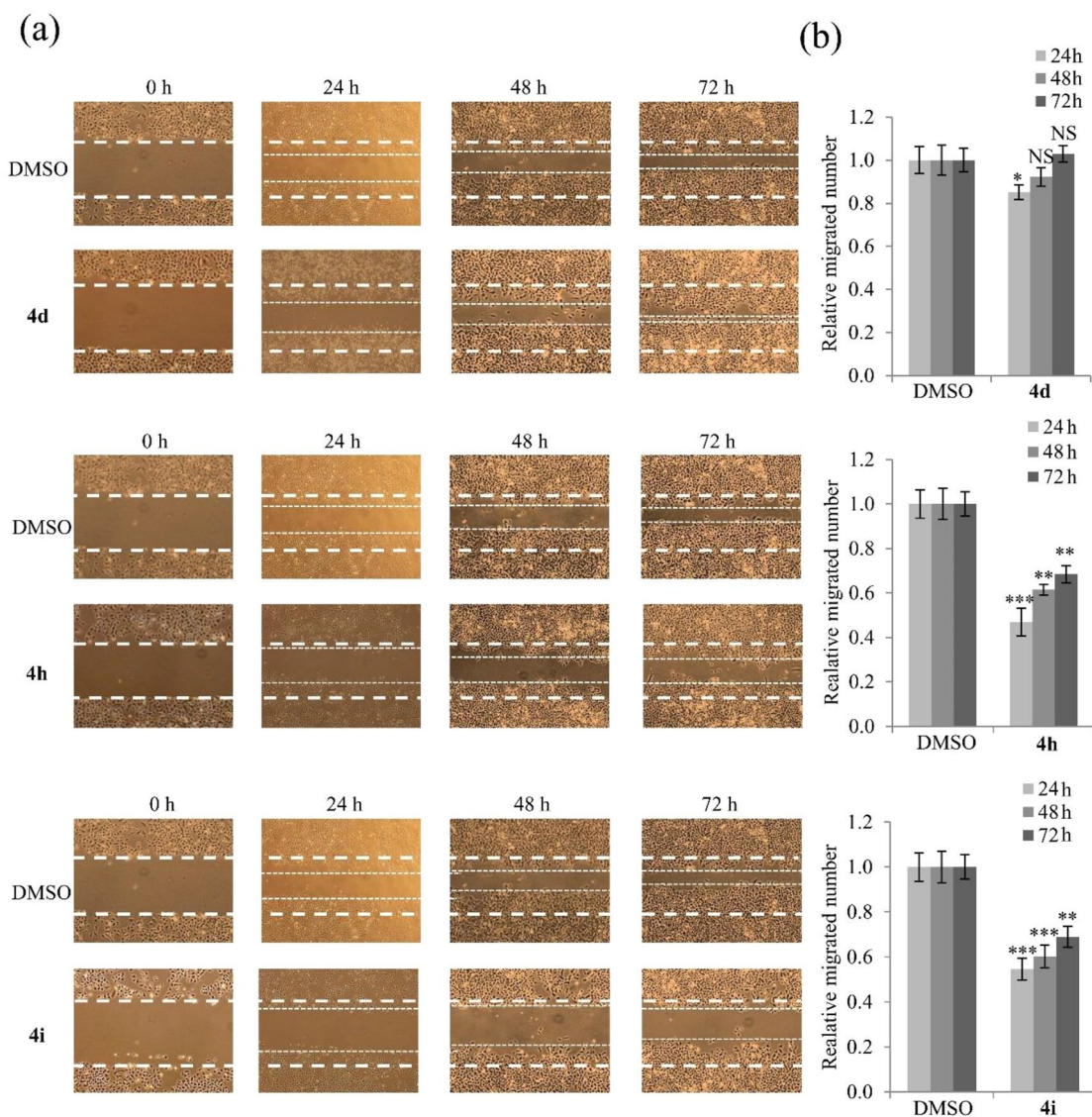


**Figure 5.** Inhibition of A549 cell migration by compounds **4d**, **4h**, and **4i**. (a) Representative images and (b) quantitative analysis of migration assays of A549 cells treated with 15  $\mu$ M compounds **4d**, **4h**, and **4i** for 24, 48, and 72 h. Representative images from three independent experiments are shown ( $n=3$ ). Data represent the mean  $\pm$  SD. \* $p < 0.05$ ; \*\* $p < 0.01$ ; \*\*\* $p < 0.001$ ; NS, no significant difference compared with DMSO-treated A549 cells.

**General procedure for the preparation of 3-aminocoumarins (4a–4j).** 3-Amino-4-hydroxycoumarin (**3**, 90 mg, 0.5 mmol) was dissolved in  $\text{CH}_2\text{Cl}_2$ . Pyridine (120  $\mu$ L, 1.5 mmol) was then added, and the mixture was cooled to 0  $^\circ\text{C}$ . Various substituted acid chloride (**4a–4j**) was added dropwise at 0  $^\circ\text{C}$ , and the mixture was stirred overnight at room temperature. The reaction mixture was evaporated and purified by column chromatography (Hexane/EtOAc, 9:1) to give the compounds 3-aminocoumarins (**4a–4j**). The yield of 10 compounds is over 80%. NMR and LC–MS spectra were obtained using a JEOL 400 MHz NMR spectrometer (JEOL, Ltd., Tokyo, Japan) and LC–MS spectrometer (Agilent Technologies, Santa Clara, CA, USA), respectively (Supplementary Fig. S5).

**Compd. 4a:** 2-ethoxy-*N*-(4-hydroxy-2-oxo-2*H*-chromen-3-yl)benzamide.  $^1\text{H NMR}$  (400 MHz,  $\text{CDCl}_3$ )  $\delta$ : 11.06 (s, NH), 8.27 (d,  $J=7.6$  Hz, 1H), 8.04 (d,  $J=7.6$  Hz, 1H), 7.569–7.50 (m, 2H), 7.35–7.30 (m, 2H), 7.13–7.05 (m, 2H), 4.37–4.32 (m, 2H), 1.72–1.68 (m, 3H).  $^{13}\text{C NMR}$  (100 MHz,  $\text{CDCl}_3$ )  $\delta$ : 165.35, 161.11, 157.80, 153.41, 150.79, 134.73, 132.64, 131.52, 124.54, 121.33, 118.70, 117.56, 116.22, 112.46, 105.57, 65.81, 14.73. LC–MS (ESI+): Calc. for  $\text{C}_{18}\text{H}_{15}\text{NO}_5$   $[\text{M} + \text{H}]^+$ : 326.10, Found: 326.2.

**Compd. 4b:** *N*-(4-hydroxy-2-oxo-2*H*-chromen-3-yl)-4-methoxybenzamide.  $^1\text{H NMR}$  (400 MHz,  $\text{CDCl}_3$ )  $\delta$ : 8.80 (s, NH), 8.03 (d,  $J=6.8$  Hz, 1H), 7.94 (d,  $J=6.8$  Hz, 1H), 7.55–7.53 (t, 2H), 7.38–7.33 (t, 2H), 7.01–6.99 (d,  $J=6.8$  Hz, 2H), 3.90 (s, 3H).  $^{13}\text{C NMR}$  (100 MHz,  $\text{CDCl}_3$ )  $\delta$ : 166.98, 163.75, 161.41, 152.72, 150.54, 131.71, 129.78, 124.80, 124.52, 123.60, 117.33, 116.34, 114.42, 104.95, 55.70. LC–MS (ESI+): Calc. for  $\text{C}_{17}\text{H}_{14}\text{NO}_5$   $[\text{M} + \text{H}]^+$ : 312.09, Found: 312.2.

**Compd. 4c:** 2-chloro-*N*-(4-hydroxy-2-oxo-2*H*-chromen-3-yl)benzamide.  $^1\text{H NMR}$  (400 MHz,  $\text{CDCl}_3$ )  $\delta$ : 9.14 (s, NH), 8.05 (d,  $J=8.4$  Hz, 1H), 7.87 (d,  $J=8.4$  Hz, 1H), 7.59–7.54 (t, 1H), 7.53–7.47 (m, 2H), 7.44–7.40 (m,

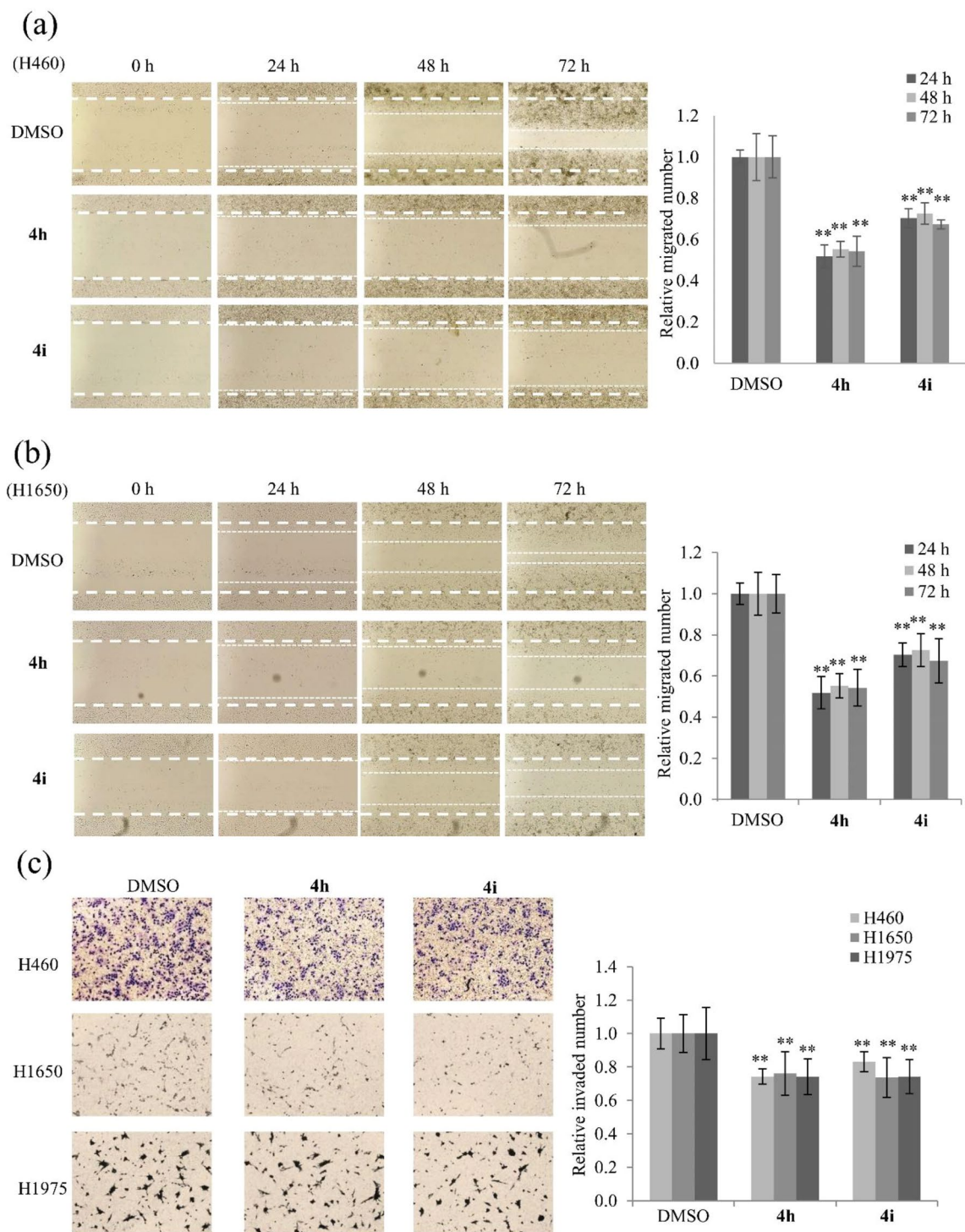


**Figure 6.** Inhibition of migration and invasion migration of different lung cancer cell lines by compounds **4h** and **4i**. **(a,b)** Representative images and quantitative analysis of migration assays of H460, and H1650 cells treated with 15  $\mu$ M of compounds **4h** and **4i** for 24, 48, and 72 h. **(c)** Representative images and quantitative analysis of invasion assays of H460, H1650, and H1975 cells treated with 15  $\mu$ M of compounds **4h** and **4i** for each cell line. Representative images from three independent experiments are shown (n = 3). Data represent the mean  $\pm$  SD. \* $p$  < 0.05, \*\* $p$  < 0.01 compared with DMSO-treated cells.

1H), 7.38–7.34 (m, 2H).  $^{13}\text{C}$  NMR (100 MHz,  $\text{CDCl}_3$ )  $\delta$ : 166.57, 162.75, 160.98, 150.75, 133.08, 132.05, 131.91, 131.64, 131.06, 130.94, 127.51, 124.86, 124.62, 117.07, 116.40, 104.91. LC–MS (ESI+): Calc. for  $\text{C}_{16}\text{H}_{11}\text{ClNO}_4$   $[\text{M} + \text{H}]^+$ : 316.04, Found: 316.2.

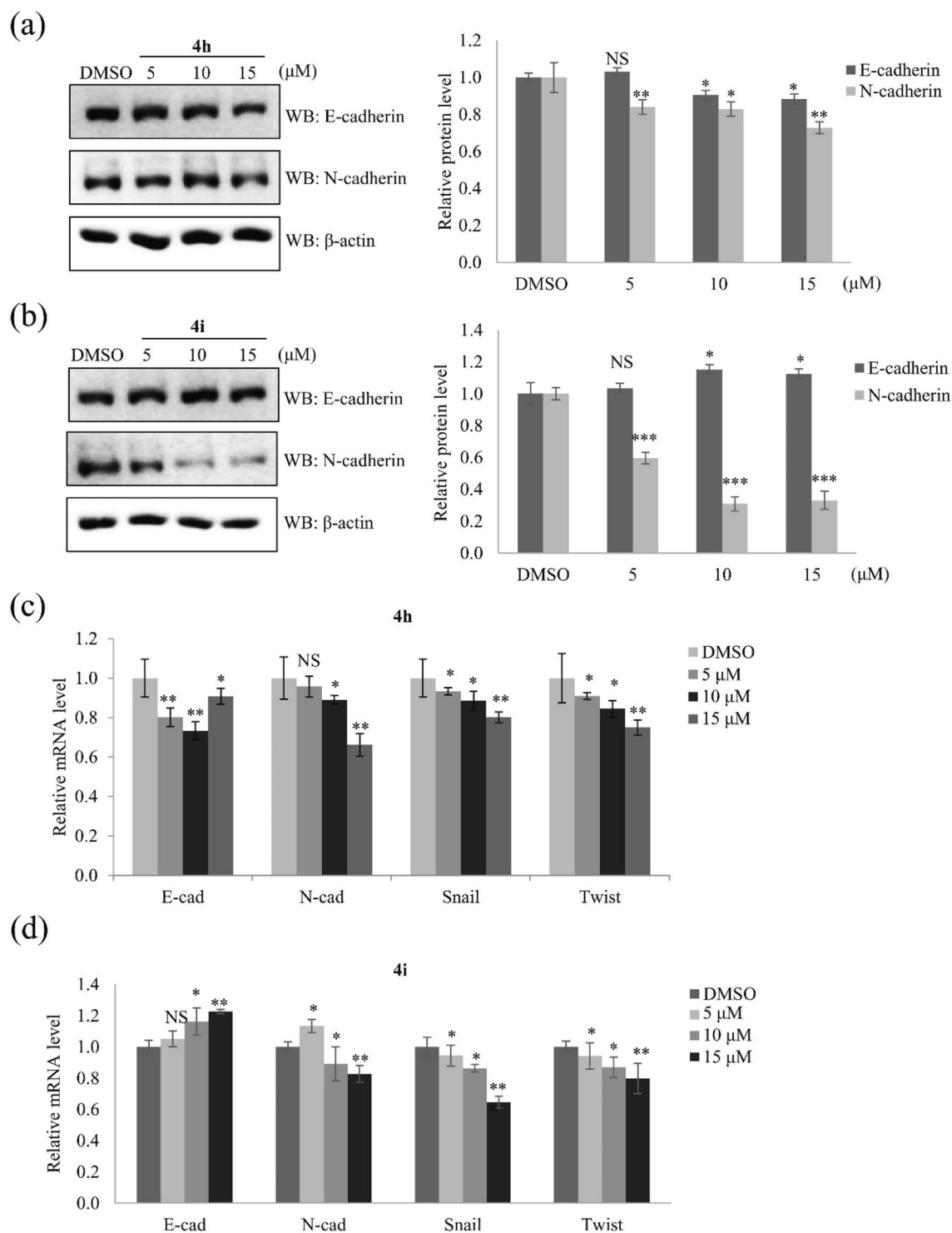


**Figure 7.** Compounds **4h** and **4i** suppress A549 cell motility by modulating expression of EMT markers and their regulators. **(a,b)** Western blotting and quantification of the relative protein levels of E-cadherin and N-cadherin in A549 cells treated with nontoxic concentrations (5, 10, and 15  $\mu\text{M}$ ) of compounds **4h** and **4i**.  $\beta$ -Actin served as a loading control. **(c,d)** Relative mRNA levels of EMT effectors (E-cadherin and N-cadherin) and their transcription factors (Snail and Twist) in A549 cells treated with nontoxic concentrations (5, 10, and 15  $\mu\text{M}$ ) of compounds **4h** and **4i**. The mRNA levels were normalized against that of the housekeeping gene GAPDH. Quantitative data were obtained from at least three independent experiments. Data represent the mean  $\pm$  SD. Statistical analysis was performed by a one-way analysis of variance. \* $p < 0.05$ ; \*\* $p < 0.01$ ; \*\*\* $p < 0.001$ ; NS, no significant difference compared with DMSO-treated A549 cells.



Compd. **4d**: *N*-(4-hydroxy-2-oxo-2*H*-chromen-3-yl)-2-methylbenzamide.  $^1\text{H NMR}$  (400 MHz,  $\text{CDCl}_3$ )  $\delta$ : 8.50 (s, NH), 8.04 (d,  $J=8.0$  Hz, 1H), 7.62 (d,  $J=8.4$  Hz, 1H), 7.58–7.56 (t, 1H), 7.490–7.30 (m, 4H), 2.61 (s, 3H).  $^{13}\text{C NMR}$  (100 MHz,  $\text{CDCl}_3$ )  $\delta$ : 170.52, 161.12, 152.87, 150.65, 137.33, 133.00, 131.90, 131.86, 131.82, 127.66, 126.38, 124.86, 124.55, 117.16, 116.37, 105.08, 20.39. LC–MS (ESI+): Calc. for  $\text{C}_{17}\text{H}_{14}\text{NO}_4$  [M + H] $^+$ : 296.09, Found: 296.2.

Compd. **4e**: *N*-(4-hydroxy-2-oxo-2*H*-chromen-3-yl)-3-methylbenzamide.  $^1\text{H NMR}$  (400 MHz,  $\text{CDCl}_3$ )  $\delta$ : 8.88 (s, NH), 8.04 (d,  $J=6.8$  Hz, 1H), 7.76–7.74 (m, 2H), 7.58–7.54 (m, 1H), 7.43–7.41 (m, 2H), 7.40–7.341 (m, 2H), 2.45 (s, 3H).  $^{13}\text{C NMR}$  (100 MHz,  $\text{CDCl}_3$ )  $\delta$ : 170.60, 167.76, 161.32, 150.61, 139.24, 134.17, 131.86, 131.52, 129.08, 128.20, 124.87, 124.78, 124.75, 116.37, 110.16, 104.86, 21.47. LC–MS (ESI+): Calc. for  $\text{C}_{17}\text{H}_{14}\text{NO}_4$  [M + H] $^+$ : 296.09, Found: 296.2.

Compd. **4f**: 4-chloro-*N*-(4-hydroxy-2-oxo-2*H*-chromen-3-yl)benzamide.  $^1\text{H NMR}$  (400 MHz,  $\text{CDCl}_3$ )  $\delta$ : 8.86 (s, NH), 8.04 (d,  $J=6.4$  Hz, 1H), 7.92 (d,  $J=8.4$  Hz, 2H), 7.59–7.55 (t, 1H), 7.53–7.50 (m, 2H), 7.39–7.34 (m, 2H).  $^{13}\text{C NMR}$  (100 MHz,  $\text{CDCl}_3$ )  $\delta$ : 166.40, 161.27, 152.96, 150.72, 141.04, 139.93, 132.03, 129.53, 129.07, 124.93, 124.59, 117.11, 116.42, 104.66. LC–MS (ESI+): Calc. for  $\text{C}_{16}\text{H}_{11}\text{ClNO}_4$  [M + H] $^+$ : 316.04, Found: 316.2.

Compd. **4g**: 4-fluoro-*N*-(4-hydroxy-2-oxo-2*H*-chromen-3-yl)benzamide.  $^1\text{H NMR}$  (400 MHz,  $\text{CDCl}_3$ )  $\delta$ : 9.66 (s, NH), 8.18–8.14 (t, 1H), 8.04 (d,  $J=7.2$  Hz, 1H), 7.64–7.60 (t, 1H), 7.58–7.54 (m, 1H), 7.38–7.33 (m, 2H), 7.26–7.23 (m, 2H).  $^{13}\text{C NMR}$  (100 MHz,  $\text{CDCl}_3$ )  $\delta$ : 163.39, 161.00, 153.07, 150.78, 135.35, 135.26, 132.20, 131.93, 125.33, 124.77, 124.59, 117.16, 116.86, 116.62, 116.40, 105.08. LC–MS (ESI+): Calc. for  $\text{C}_{16}\text{H}_{11}\text{FNO}_4$  [M + H] $^+$ : 300.07, Found: 300.2.

Compd. **4h**: 3-chloro-*N*-(4-hydroxy-2-oxo-2*H*-chromen-3-yl)benzamide.  $^1\text{H NMR}$  (400 MHz,  $\text{CDCl}_3$ )  $\delta$ : 8.87 (s, NH), 8.05 (d,  $J=8$  Hz, 1H), 7.96 (m, 1H), 7.83 (d,  $J=8$  Hz, 1H), 7.61–7.55 (m, 2H), 7.50–7.46 (m, 1H), 7.9–7.35 (m, 2H).  $^{13}\text{C NMR}$  (100 MHz,  $\text{CDCl}_3$ )  $\delta$ : 166.15, 161.22, 153.03, 150.65, 135.60, 133.39, 132.08, 130.46, 128.12, 125.49, 124.94, 124.61, 116.43. LC–MS (ESI+): Calc. for  $\text{C}_{16}\text{H}_{11}\text{ClNO}_4$  [M + H] $^+$ : 316.04, Found: 316.2.

Compd. **4i**: *N*-(4-hydroxy-2-oxo-2*H*-chromen-3-yl)-[1,1'-biphenyl]-4-carboxamide.  $^1\text{H NMR}$  (400 MHz,  $\text{CDCl}_3$ )  $\delta$ : 8.95 (s, NH), 8.05–8.02 (m, 3H), 7.76 (d,  $J=8.8$  Hz, 2H), 7.65 (d,  $J=8.8$  Hz, 2H), 7.59–7.54 (m, 1H), 7.50–7.47 (m, 2H), 7.44–7.35 (m, 3H).  $^{13}\text{C NMR}$  (100 MHz,  $\text{CDCl}_3$ )  $\delta$ : 167.19, 161.35, 152.93, 150.61, 146.23, 139.52, 131.88, 130.07, 129.14, 128.58, 128.25, 127.78, 127.38, 124.87, 124.58, 117.24, 116.39, 104.87. LC–MS (ESI+): Calc. for  $\text{C}_{22}\text{H}_{16}\text{NO}_4$  [M + H] $^+$ : 358.11, Found: 358.2.

Compd. **4j**: 2-fluoro-*N*-(4-hydroxy-2-oxo-2*H*-chromen-3-yl)benzamide.  $^1\text{H NMR}$  (400 MHz,  $\text{CDCl}_3$ )  $\delta$ : 8.05–8.01 (m, 2H), 7.60–7.54 (m, 2H), 7.25–7.14 (m, 4H).  $^{13}\text{C NMR}$  (100 MHz,  $\text{CDCl}_3$ )  $\delta$ : 169.89, 164.01, 161.41, 135.66, 135.57, 132.83, 124.20, 124.16, 117.87, 117.79, 117.35, 117.12. LC–MS (ESI+): Calc. for  $\text{C}_{16}\text{H}_{11}\text{FNO}_4$  [M + H] $^+$ : 300.07, Found: 300.2.

**Biological evaluation.** *Cell culture and material.* The lung cancer cell lines A549, H1650, H1975, and H460 were obtained from the Korean Cell Line Bank (Seoul, South Korea). Cells were cultured in RPMI 1640/DMEM culture medium (Gen Depot, TX, USA) supplemented with 10% fetal bovine serum (Gen Depot, TX, USA) and 1% Penicillin–Streptomycin solution. Cells were cultured in 5%  $\text{CO}_2$  in a humidified atmosphere at 37 °C. 4-Hydroxycoumarin was purchased from Sigma-Aldrich (H23805).

*MTT assay.* Cells ( $2 \times 10^4$  cells/well) were seeded on a 96-well plate, grown overnight, and then treated with 4-hydroxycoumarin and its derivatives **4a–4j** at concentrations from 3.125 to 100  $\mu\text{M}$  for 48 h. After incubation with MTT at 37 °C, cells were lysed with 150  $\mu\text{L}$  of DMSO (Sigma-Aldrich, St. Louis, USA) and absorbance was measured spectrophotometrically at 540 nm.

*Invasion assay.* Invasion assays were performed in Transwell chambers (Corning, New York, USA) with 8  $\mu\text{m}$  pore size polycarbonate membrane coated with 1% gelatin. A549, H1650, H1975, and H460 cells were plated at  $2 \times 10^6$  cells/mL in RPMI1640 containing 0.2% bovine serum albumin (BSA) in the upper compartment of the chamber. The lower chamber was filled with 400  $\mu\text{L}$  RPMI containing 0.2% BSA and 10  $\mu\text{g}/\text{mL}$  fibronectin (EMD MilliporeCorp., Billerica, MA, USA) as a chemoattractant. A549 cells were treated with 5  $\mu\text{M}$  of 4-hydroxycoumarin and its derivatives (**4a–4j**) for 48 h. H1650, H1975, and H460 cells were treated with 5, 10, and 15  $\mu\text{M}$  of derivatives **4h** and **4i** for 48 h. After incubation, the cells in the upper chamber were fixed with Diff Quik kit (Sysmex, Kobe, Japan). The numbers of cells in five fields per chamber were counted using a Nikon Eclipse 400fluorescence microscope (Nikon Instech, Co., Ltd, Kawasaki, Japan) and iSolution FL Auto  $\times 64$  software (IMT iSolution Inc., Vancouver, Quebec, Canada).

*Wound healing assay.* A549, H460, and H1650 cells were plated at a density of  $2.5 \times 10^5$  cells/well and grown overnight to the confluence. Monolayer cells were scratched to create a wound. The cells were then washed twice and incubated in RPMI1640 culture medium supplemented with 2% FBS with 15  $\mu\text{M}$  of derivatives **4d**, **4h**, and **4i**. For the quantitation of relative migration ability, photographs of cells were taken at 0, 24, 48, and 72 h after wounding to measure the width of the wound. The distance migrated by the cells was calculated as the difference between the edges of the wound at time point 1 and at time point 2. For each sample, an average of five wound distances was taken to determine the average rate of migration at the time-course of 24, 48, and 72 h. The migrating rate was determined with the following formula: migrating rate [%] = (width t1 [mm] – width t2 [mm]) / width t1  $\times 100\%$ .

*Western blots.* A549 cells were treated with 5, 10, or 15  $\mu\text{M}$  concentrations of compounds **4d**, **4h** and **4i** for 24 h. Cells were lysed and the proteins (25  $\mu\text{g}$ ) were separated by 10% polyacrylamide gel electrophoresis containing 0.1% SDS and electrophoretically transferred to nitrocellulose membranes. Anti-E-cadherin (#3195) (Cell signaling) and anti-N-cadherin(#13A9) (Cell signaling) were used as primary antibodies for the detec-



tion of EMT markers. Anti- $\beta$ -actin (Santa Cruz Biotechnology) was used as internal standards. All results are representative from at least three independent experiments. Bands were measured by Multi Gauge version 3.0 (Fuji photo film Co., Ltd., Tokyo, Japan) and their relative density calculated based on the density of the  $\beta$ -actin bands in each sample. Values were expressed as arbitrary densitometric units corresponding to signal intensity. Cropped gels retain important bands, but whole gel images with membrane edges visible are available in Supplementary Figs. S3 and S4.

**qRT-PCR.** Briefly, total RNA was isolated from compounds **4h** or **4i** treated A549 cells using RNAiso Plus (TaKaRa, Otsu, Shiga 520-2193, Japan) and then total RNAs (1  $\mu$ g) were used to synthesize cDNA using a M-MLV reverse transcriptase kit (Invitrogen, Carlsbad, CA, USA) and SYBR green (Enzymomics, Seoul, Korea). qRT-PCR reactions and analysis were performed using CFX (Bio-Rad, Hercules, CA, USA). The primers used for real-time PCR were as follows: E-cadherin (forward) 5'-cagaaagtgtccaccaaaag-3' and (reverse) 5'-aaatgtgag-caattctgctt-3'; N-cadherin (forward) 5'-ctcctatgagtgaacaggaacg-3' and (reverse) 5'-ttggatcaatgataatcaatgctgtgta-3'; Snail (forward) 5'-tcccgggcaatttaacaatg-3' and (reverse) 5'-tgggagacacatcggtcga-3'; Twist (forward) 5'-cgggagtcgcagcttcta-3' and (reverse) 5'-tgaatctgctcagctgtgc-3'; and GAPDH (forward) 5'-atccatcttccag-gagcga-3' and (reverse) 5'-agttgcatgtagacacctggc-3'. Target gene expression was normalized relative to the expression of GAPDH in the same sample.

**Statistical analysis.** All in vitro experiments were performed in triplicate. Data are presented as the mean standard deviation (SD) of 3 independent experiments with 3 replicates each. The student's t-test was utilized to determine statistical significance between two groups, and analysis of variance was utilized between three or more groups, respectively. Values of  $p < 0.05$  were considered statistically significant. All statistical analyses were performed using Sigma Plot 12.5 software (Systat software, Erkrath, Germany).

### Data availability

All data generated or analyzed during this study are included in this published article and its supplementary information file.

Received: 3 June 2022; Accepted: 12 December 2022

Published online: 14 December 2022

### References

- Roser, M. & Ritchie, H. *Cancer*. <https://ourworldindata.org/cancer/> (2015).
- Sung, H. *et al.* Global cancer statistics 2020: GLOBOCAN estimates of incidence and mortality worldwide for 36 cancers in 185 countries. *CA Cancer J. Clin.* **71**, 209–249 (2021).
- Zhu, X., Chen, J., Yang, F. & Tang, C. Multiple sites of soft-tissue metastases secondary to lung cancer: A case report. *Medicine (Baltimore)* **98**, e18162 (2019).
- Zappa, C. & Mousa, S. A. Non-small cell lung cancer: Current treatment and future advances. *Transl. Lung Cancer Res.* **5**, 288 (2016).
- Mittal, V. Epithelial mesenchymal transition in aggressive lung cancers. *Adv. Exp. Med. Biol.* **890**, 37–56 (2016).
- Li, Z. *et al.* lncRNA PCBP1-AS1 correlated with the functional states of cancer cells and inhibited lung adenocarcinoma metastasis by suppressing the EMT progression. *Carcinogenesis* **42**, 931–939 (2021).
- Adimule, V. M., Nandi, S. S., Kerur, S., Khadapure, S. A. & Chinnam, S. J. Recent advances in the one-pot synthesis of coumarin derivatives from different starting materials using nanoparticles: A review. *Top. Catal.* <https://doi.org/10.1007/s11244-022-01571-z> (2022).
- Khursheed, A. & Jain, V. Medicinal research progress of natural coumarin and its derivatives. *Nat. Prod. J.* **11**, 648–662 (2021).
- Hu, X. L., Xu, Z., Liu, M. L., Feng, L. S. & Zhang, G. D. Recent developments of coumarin hybrids as anti-fungal agents. *Curr. Top. Med. Chem.* **17**, 3219–3231 (2017).
- Gao, F., Xiao, J. & Huang, G. Current scenario of tetrazole hybrids for antibacterial activity. *Eur. J. Med. Chem.* **184**, 111744 (2019).
- Thomas, V., Giles, D., Basavarajaswamy, G., Kumar Das, A. & Patel, A. Coumarin derivatives as anti-inflammatory and anticancer agents. *Anticancer Agents Med. Chem.* **17**, 415–423 (2017).
- Song, X. F., Fan, J., Liu, L., Liu, X. F. & Gao, F. Coumarin derivatives with anticancer activities: An update. *Arch. Pharm. (Weinheim)* **353**, 2000025 (2020).
- Turkecul, K., Colpan, R. D., Baykul, T., Ozdemir, M. D. & Erdogan, S. J. Esculetin inhibits the survival of human prostate cancer cells by inducing apoptosis and arresting the cell cycle. *J. Cancer Prev.* **23**, 10 (2018).
- Patil, J. R. *et al.* 5-Geranyloxy-7-methoxycoumarin inhibits colon cancer (SW480) cells growth by inducing apoptosis. *Planta Med.* **79**, 219–226 (2013).
- Song, J. *et al.* Discovery of novel coumarin-indole derivatives as tubulin polymerization inhibitors with potent anti-gastric cancer activities. *Eur. J. Med. Chem.* **238**, 114467 (2022).
- Gong, L. *et al.* Design, synthesis and biological evaluation of coumarin derivatives as NEDD8 activating enzyme inhibitors in pancreatic cancer cells. *Med. Chem.* **18**, 679–693 (2022).
- Lončarić, M., Gašo-Sokač, D., Jokić, S. & Molnar, M. Recent advances in the synthesis of coumarin derivatives from different starting materials. *Biomolecules* **10**, 151 (2020).
- Aslam, K., Khosa, M. K., Jahan, N. & Nosheen, S. Short communication: Synthesis and applications of coumarin. *Pak. J. Pharm. Sci.* **23**, 449–454 (2010).
- Ganesh, K. & Massagué, J. Targeting metastatic cancer. *Nat. Med.* **27**, 34–44 (2021).
- Bray, F. *et al.* Global cancer statistics 2018: GLOBOCAN estimates of incidence and mortality worldwide for 36 cancers in 185 countries. *CA Cancer J. Clin.* **68**, 394–424 (2018).
- Stuelten, C. H., Parent, C. A. & Montell, D. J. Cell motility in cancer invasion and metastasis: Insights from simple model organisms. *Nat. Rev. Cancer* **18**, 296–312 (2018).
- Pijuan, J. *et al.* In vitro cell migration, invasion, and adhesion assays: From cell imaging to data analysis. *Front. Cell Dev. Biol.* **7**, 107 (2019).
- Martinotti, S. & Ranzato, E. Scratch wound healing assay. *Methods Mol. Biol.* [https://doi.org/10.1007/7651\\_2019\\_259](https://doi.org/10.1007/7651_2019_259) (2019).

24. Loh, C. Y. *et al.* The E-cadherin and N-cadherin switch in epithelial-to-mesenchymal transition: Signaling, therapeutic implications, and challenges. *Cells* **8**, 1118 (2019).
25. Xiao, D. & He, J. Epithelial mesenchymal transition and lung cancer. *J. Thorac. Dis.* **2**, 154 (2010).
26. Chen, L. T., Zhu, K. B. & Qu, C. F. Novel 4-hydroxycoumarin derivatives: Inhibiting growth of human lung cancer cells. *Main Group Met. Chem.* **17**, 301–307 (2018).
27. Sinkevicius, K. W. *et al.* E-cadherin loss accelerates tumor progression and metastasis in a mouse model of lung adenocarcinoma. *Am. J. Respir. Cell Mol. Biol.* **59**, 237–245 (2018).
28. Quintanal-Villalonga, Á. *et al.* The FGFR4-388arg variant promotes lung cancer progression by N-cadherin induction. *Sci. Rep.* **8**, 1–13 (2018).

## Acknowledgements

This work was supported by the National Research Foundation of Korea Grant (NRF-2020R1C1C1007832) funded by the Korea government (MSIP).

## Author contributions

H.K. and H.H.H. conceived and designed the experiments. R.Z. and Y.H.Y. performed the experiments. R.Z. and H.K. analyzed the data and wrote the manuscript. All authors read and approved the final manuscript. All authors read the M.S. and are agree with submission in its present for to the journal of Scientific Reports. The M.S. is original and is not considered for publication by other journals.

## Competing interests

The authors declare no competing interests.

## Additional information

**Supplementary Information** The online version contains supplementary material available at <https://doi.org/10.1038/s41598-022-26212-z>.

**Correspondence** and requests for materials should be addressed to H.K. or H.-H.H.

**Reprints and permissions information** is available at [www.nature.com/reprints](http://www.nature.com/reprints).

**Publisher's note** Springer Nature remains neutral with regard to jurisdictional claims in published maps and institutional affiliations.



**Open Access** This article is licensed under a Creative Commons Attribution 4.0 International License, which permits use, sharing, adaptation, distribution and reproduction in any medium or format, as long as you give appropriate credit to the original author(s) and the source, provide a link to the Creative Commons licence, and indicate if changes were made. The images or other third party material in this article are included in the article's Creative Commons licence, unless indicated otherwise in a credit line to the material. If material is not included in the article's Creative Commons licence and your intended use is not permitted by statutory regulation or exceeds the permitted use, you will need to obtain permission directly from the copyright holder. To view a copy of this licence, visit <http://creativecommons.org/licenses/by/4.0/>.

© The Author(s) 2022